Thermal conductivity of textile reinforcements for composites

Yue El-Hage[1], Simon Hind[2], and François Robitaille[1] (ORCID)

Abstract

Thermal conductivity data for dry carbon fibre fabrics are required for modelling heat transfer during composites manufacturing processes; however, very few published data are available. This article reports in-plane and through-thickness thermal conductivities measured as a function of fibre volume fraction (V_f) for non-crimp and twill carbon reinforcement fabrics, three-dimensional weaves and reinforcement stacks assembled with one-sided carbon stitch. Composites made from these reinforcements and glass fibre fabrics are also measured. Clear trends are observed and the effects of V_f, de-bulking and vacuum are quantified along with orthotropy ratios. Limited differences between the conductivity of dry glass and carbon fibre fabrics in the through-thickness direction are reported. An unexpected trend in the relationship between that quantity and V_f is explained summarily through simple simulations.

Keywords

Thermal conductivity, carbon fabrics, composite materials, three-dimensional weaves, two–dimensional weaves

Introduction

Carbon fibres offer excellent tensile properties and low densities leading to extensive use as reinforcements for composite materials. Dry textiles reinforcements are available in various types and architectures; these dry reinforcements are saturated with a polymer resin upon composites manufacturing, in a separate manufacturing stage. Knowledge of the thermal conductivity of dry reinforcements is paramount in assessing and modelling heat transfer during composites manufacturing processes such as resin film infusion (RFI) or semi-preg consolidation, as heat transfer rates through the dry reinforcements will impact the evolution of resin viscosity, consolidation and cure.

Thermal conductivity values for constituent carbon fibres are found readily in the literature [1–3] and are often reported by manufacturers. The thermal conductivity of composites made from carbon fibres was also studied extensively.[4–7] The rule of mixture (1) is widely acknowledged for predicting the longitudinal in-plane thermal conductivity λ_{cip} of unidirectional fibre-reinforced composites

$$\lambda_{\text{cip}} = V_f \cdot \lambda_{\text{fa}} + (1 - V_f) \cdot \lambda_m \tag{1}$$

where λ_{fa} is the thermal conductivity of the fibres in the axial direction and λ_m is the thermal conductivity of the matrix; the longitudinal in-plane thermal conductivity is a linear function of fibre volume fraction (V_f).[8,9] Clayton's analytical model (2) is widely used for predicting the transverse thermal conductivity of unidirectional fibre-reinforced composites from the thermal conductivity of the fibres in the transverse direction λ_{ft} [8,10] yielding a mild exponential trend as a function of V_f.[9] Clayton's model may also be used for predicting the through-thickness thermal conductivity λ_{ctt} of laminates manufactured from unidirectional plies as this is equal to the transverse conductivity of a single ply.[11]

$$\lambda_{\text{ctt}} = \frac{\lambda_m}{4} \left\{ \sqrt{(1 - V_f)^2 \left(\frac{\lambda_{\text{ft}}}{\lambda_m} - 1\right)^2 + \frac{4\lambda_{\text{ft}}}{\lambda_m}} - (1 - V_f)\left(\frac{\lambda_{\text{ft}}}{\lambda_m}\right) \right\}^2 \tag{2}$$

[1] Mechanical Engineering, University of Ottawa, Ottawa, Ontario, Canada
[2] National Research Council Canada, Aerospace Portfolio – Structures, Materials and Manufacturing, Ottawa, Ontario, Canada

Corresponding author:
François Robitaille, Mechanical Engineering, University of Ottawa, Colonel By Hall, 161 Louis Pasteur, Ottawa, Ontario, Canada K1 N 6N5.
Email: francois.robitaille@uottawa.ca

Conversely, little is known about the thermal conductivity of dry carbon fibre reinforcements. One source reports the through-thickness thermal conductivity λ_{rtt} of a T300 carbon fibre plain weave as 0.074 W m^{-1} K^{-1} with no stated V_f; an analytical model was proposed using an electric circuit analogy.[12] No computational models for the thermal conductivity of dry fabrics are available in the open literature. The clothing industry has studied thermal insulation for textiles such as woven cotton in a broad sense[13] but no studies were published on the effect of V_f and few on the effect of fabric architecture.[14,15]

This article features results from four series of tests. Test series 1 probes the effects of textile architecture, de-bulking, vacuum and V_f on the in-plane and through-thickness thermal conductivity of dry reinforcements, λ_{rip} and λ_{rtt}, for two reinforcements made of the same carbon fibres. Composites were produced from the same reinforcements; λ_{cip} and λ_{ctt} were measured for comparison purposes. Test series 2 quantifies the effects of textile architecture, thickness and nature of yarns extending along the thickness for three monolithic three-dimensional (3D) woven dry reinforcements. Tests were conducted at a single V_f for each reinforcement given their relative stiffness along the thickness; composites were produced and tested. Test series 3 probes the effect of stitching a stack of carbon reinforcement through its entire thickness with a structural 134 tex twisted carbon thread using a single-sided stitching head; λ_{rip} and λ_{rtt} were measured at different V_f values. Finally, test series 4 probes the effects of V_f on λ_{rip} and λ_{rtt} for one dry glass fibre reinforcement and glass fibre composite, enabling comparisons with results obtained in test series 1 to 3.

Thermal conductivity of carbon fibres

Carbon fibres derived from polyacrylonitrile (PAN) precursors offer excellent tensile strength but have relatively low thermal conductivity. Typical axial thermal conductivities λ_{fa} for these fibres range from 7 W m^{-1} K^{-1} to 10 W m^{-1} K^{-1}; however, values vary within a wide range from 4 W m^{-1} K^{-1} to 180 W m^{-1} K^{-1} as reported by Beckwith.[16] Pitch-based carbon fibres offer improved stiffness and drastically increased thermal and electrical conductivity, at the expense of reduced tensile strength compared with PAN-based fibres. λ_{fa} for pitch-based fibres generally range from 10 W m^{-1} K^{-1} to 600 W m^{-1} K^{-1} [7,17]: Zweben[18] reported a maximum value of 1100 W m^{-1} K^{-1} from literature; Glowania et al.[7] reported up to 800 W m^{-1} K^{-1}. Vapour-grown carbon fibres are produced in short lengths of 50 mm to 70 mm and diameters as small as 0.1 μm from the vapour of low molecular weight hydrocarbon compounds.[19] Their commercialization in the 1990s placed more emphasis on enhancing properties such as electrical and thermal conductivity, where values up to 2000 W m^{-1} K^{-1} were reported on a pilot scale.[18,20,21]

Hou et al.[22] measured the thermal diffusivity of a single PAN-based fibre at 1.15×10^{-7} m^2 s^{-1} using optical heating and electrical thermal sensing techniques. Wei[23] reported λ_{fa} values for T300 and another unspecified PAN-based fibre to be 4.9 and 4.4 W m^{-1} K^{-1}, respectively, using the laser flash method, compared with 10.5 W m^{-1} K^{-1} cited by the manufacturer for T300. The effect of heat treatment temperature was probed: Katzman et al.[24] reported λ_{fa} values ranging from 2 W m^{-1} K^{-1} to 14 W m^{-1} K^{-1} for PAN-based fibres at different heat treatment temperatures, while Qiu et al.[25] measured λ_{fa} using a modified 3-ω technique and obtained values ranging from 20 W m^{-1} K^{-1} to 69 W m^{-1} K^{-1} from a single PAN-based fibre heat treated at 1500°C to 2100°C.

The effect of temperature on thermal conductivity was also investigated. Yamane et al.[1] calculated λ_{fa} of a single PAN-based fibre ranging from 300 to 800 K from measured thermal diffusivities. The authors studied five MJ series high stiffness PAN-based fibres and two T series high strength PAN-based fibres from Toray. λ_{fa} values ranged from 5 W m^{-1} K^{-1} to 180 W m^{-1} K^{-1} as a function of temperature. Values for high strength fibres were within typical values for PAN-based fibres cited above, while those for the high stiffness fibres were some of the highest reported for PAN-based fibres. Correlations were often found relating thermal conductivity of carbon fibres to their stiffness, as stiffness is directly dependent on the fibre microstructure.[1]

Various data sheets for PAN-based carbon fibres are available from suppliers. Values of λ_{fa} reported by Hexcel for fibres IM7, IM10 and AS4 are 5.4, 6.1 and 6.8 W m^{-1} K^{-1}, respectively.[26–28] Toho Tenax cited λ_{fa} for both HTS40 and HTS45 fibres at 10 W m^{-1} K^{-1}.[29] Toray cited 10.5 W m^{-1} K^{-1} for λ_{fa} of fibre T300[30], while BP Amoco cited 14 and 15 W m^{-1} K^{-1} for fibres T650/35 and T650/42, respectively.[31]

Published data for the transverse fibre thermal conductivity λ_{ft} are sparse. Values for PAN-based carbon fibres are often estimated through orthotropy ratios where λ_{ft} is generally 5 to 10 times lower than λ_{fa}[8] or back-calculated using various analytical models given V_f and the through-thickness thermal conductivity of a composite plate λ_{ctt} made from the same fibre.[32] The only λ_{ft} values cited by suppliers are 5 W m^{-1} K^{-1} for both T650/35 and T650/42 fibres from BP Amoco.[31] Bol'shakova et al.[33] published the only paper reporting λ_{fa} as well as λ_{ft} for several carbon fibres. Measurements were done over temperatures ranging from 0°C to 600°C in either air or oil. Values of λ_{fa} and λ_{ft} are not directly comparable as the fibres used had different densities. Still, results lead to orthotropy ratios of approximately 15 for a PAN-based carbon fibre and 40 for a pitch-based fibre at room temperature. For the PAN-based fibre, λ_{fa} remained approximately constant at different temperatures while λ_{ft} increased approximately linearly as a function of temperature.

Although most thermal conductivities reported for PAN-based fibres are low, some fibres returned higher values, such as the MJ series reported above and Thornel

50 with λ_{fa} of 70 W m^{-1} K^{-1} as cited by Cytec[34]; Lee and Taylor[3] measured 59 W m^{-1} K^{-1} for the same fibre using the laser flash method. Generally, common grade commercial PAN-based carbon fibre can be expected to return λ_{fa} values in the range of 10–20 W m^{-1} K^{-1}.

Thermal conductivity of carbon fibre textile reinforcements

Most data found for the thermal conductivity of textiles originate from the clothing industry for applications such as firefighter clothing or insulation for winter jackets. Matusiak[13] studied the thermal insulation of single and multilayered textile materials and concluded that porous non-woven materials offer high thermal diffusion. Uzun[35] measured the thermal conductivity of fabrics made of natural fibres. Onofrei et al.[14] conducted studies on the effect of knit structure on the thermal conductivity of fabrics made of thermoregulating yarns. Thermal conductivity was measured for nine different knitted structures; some knit structures were found to offer higher thermal conductivity than others. Matusiak and Sikorski[15] studied the effect of fabric architecture by measuring thermal conductivity of plain, twill 1/3, twill 2/2, rep 1/1, rep 2/2 and hopsack 2/2 cotton fabric weaves. The plain weave fabric yielded higher thermal conductivity which the authors attributed to its higher density, followed by the twill 1/3 and rep 2/2, while the hopsack 2/2 yielded lower thermal conductivity. The authors concluded that the effect of weave type was statistically significant.

A few articles reported on the general heat transfer behaviour of woven fabrics. Xiaogang et al.[36] investigated heat conduction in PAN-based carbon fibre fabrics based on infrared imaging. They obtained temperature-time curves for five different fabrics. Ziaei and Ghane[37] studied the thermal insulation properties of cotton and polyester spacer fabrics impregnated with ceramic powders, which effectively reduced the thermal conductivity of these fabrics. The authors stated that natural convection in porous materials with densities higher than 20 kg m^{-3} is negligible and that since the thermal conductivity of air is much lower than that of the fibres, air between the fibres plays an important role in determining the thermal properties of textiles.

Even fewer studies were performed by the composites or aerospace industry aiming at studying the in-plane thermal conductivity λ_{rip} or through-thickness thermal conductivity λ_{rtt} of dry carbon fibre fabrics. Yamashita et al.[38] measured the transverse thermal conductivity of T300 carbon fibres as well as that of plain woven reinforcement made from the same fibre, and fibre-epoxy composite made from the same textile. Values of λ_{ft}, λ_{rtt} and λ_{ctt} were measured as 0.095, 0.074 and 0.302 W m^{-1} K^{-1}, respectively; the authors reported no corresponding V_f values for these measurements. Two models were developed for predicting the through-thickness thermal conductivity of the

reinforcement and composite using an electric circuit analogy, with predictions made over V_f values ranging from 20 to 50%. For the reinforcement, predicted λ_{rtt} values ranged from 0.05 W m^{-1} K^{-1} to 0.08 W m^{-1} K^{-1}, varying linearly with V_f. The authors attributed the increase in content of high thermal conductivity fibres without further explanation to the linear trend. For the composite, thermal conductivity values in the through-thickness direction λ_{ctt} ranged from 0.21 W m^{-1} K^{-1} to 0.25 W m^{-1} K^{-1} and remained constant with V_f, which is unexpected for carbon fibre-epoxy composites.

Bol'shakova et al.[33] measured λ_{rip} of graphite fibre textile TGN-2 M and λ_{rtt} of carbon fibre textile Ural T-22 as a function of temperature in different mediums of air, nitrogen and vacuum. The authors did not state corresponding V_f values for these measurements. Thermal conductivity in air in both directions increased with temperature with λ_{rip} values ranging from 0.6 W m^{-1} K^{-1} to 1.4 W m^{-1} K^{-1} following an exponential recovery trend and λ_{rtt} values ranging from 0.22 W m^{-1} K^{-1} to 0.28 W m^{-1} K^{-1} following a linear trend. Comparing thermal conductivity in air in the in-plane and through-thickness directions yielded orthotropy ratios of approximately 3; however, the data cannot be compared directly since the measurements resulted from fabrics of different densities made from different fibres, with unspecified textile architecture. It was also observed that the through-thickness thermal conductivity of reinforcements was affected significantly when experiments were conducted in air and under vacuum. As for reinforcement data from suppliers, Cytec cited a λ_{rtt} value of 0.25 W m^{-1} K^{-1} for Thornel VCB-20 carbon fibre cloth while stating that λ_{fa} for the constituent carbon fibre was 15 W m^{-1} K^{-1}.[39] Hes and Dolezal[40] developed the LAMBDATEST device which measures thermal conductivities ranging from 1 W m^{-1} K^{-1} to 200 W m^{-1} K^{-1}, so it may be used in probing carbon fibre textile and composites.

Results featured herein include λ_{rip} and λ_{rtt} data measured using dedicated equipment, where the effects of reinforcement architecture and V_f are documented systematically for textile reinforcements made from fibres of known conductivities λ_{fa} and λ_{ft}. Orthotropy ratios for the fabrics are quantified and compared with those of the constituent fibres. Variability induced by repeated measurements performed on different samples and by the apparatus are quantified along with the effect of dry samples being enclosed within a film as part of the measurement technique. The conductivity of samples subjected to repeated compaction cycles and to vacuum is probed as both cases are relevant to manufacturing processes for composites, along with the effect of modern preform construction techniques including carbon thread stitching and the use of monolithic, thick 3D textile reinforcements. Conductivity data obtained from composites made from the same reinforcements, and from glass fibre reinforcements, are also included for comparison purposes. Trends are identified and limitations of models developed for predicting

Figure 1. THISYS and THASYS thermal conductivity apparatus with bagged dry reinforcement samples.

the conductivity of composites as opposed to dry reinforcement fabrics are highlighted. Preliminary computational models are offered aiming at providing a first explanation for some of the trends derived from experimental results.

Experimental

Devices, materials and sample preparation

Dedicated thermal conductivity measurement devices THISYS and THASYS manufactured by Hukseflux were used for experimental data collection, Figure 1. THISYS and THASYS measure in-plane and through-thickness thermal conductivities, respectively, requiring one or two flat samples measuring approximately 70 mm × 110 mm. Detailed information about the configuration and operation of the devices appears in.[8] The technique used for obtaining directional in-plane conductivity values was not used here as all samples were thermally quasi-isotropic in their plane; bulk in-plane thermal conductivities were measured as envisaged by Hukseflux in regular operation.

THISYS and THASYS rely on immersing the heat source, heat sink and solid samples in glycerol to reduce contact thermal resistances and improve measurement accuracy. While the devices are typically used for measuring in-plane λ_{cip} and through-thickness λ_{ctt} thermal conductivities of solid materials, in this work, they were also used for measuring the in-plane λ_{rip} and through-thickness λ_{rtt} thermal conductivities of dry textile reinforcements in air and under vacuum. Dry fabrics, which are detailed below, were cut into 70 mm × 110 mm plies, stacked and sealed into 50 μm thick Dahlar® release film 125 from Airtech. Each sealed dry reinforcement sample was tested for leaks by immersion in water for 10 min, to avoid penetration of glycerol from the devices into the dry fabric samples during measurement. Most samples were sealed on three sides leaving the top side open to enable progressive compaction and increase in V_f of the samples in the devices. Samples measured under vacuum were sealed on all sides and

equipped with a port sealed in the release film for connection to a Gast DAA-V715A vacuum pump set to 0.02 bar absolute, Figure 1.

Dry samples in test series 1, 3 and 4 were tested at different V_f to capture the evolution of λ_{rip} and λ_{rtt} in reinforcements subjected to typical consolidation profiles upon composites manufacturing. All samples mounted between spring-loaded heater plates with adjustable spacing were compacted to precise V_f values using accurately milled spacers of low thermal conductivity inserted away from heat transfer pathways in the devices. Inserts with five thicknesses ranging from 4.76 mm to 3.39 mm enabled V_f values ranging generally from 35% to 60%; these values correspond to reinforcements as received and subjected to compaction pressures typical of composites manufacturing processes. Samples were brought to the highest V_f at 3.39 mm thickness by pre-compacting to 1.0 MPa at 4 mm min^{-1} using an Instron 4482 universal testing frame equipped with parallel compaction platens; all other thicknesses were reached through manual tightening in the THISYS and THASYS devices. The effect of de-bulking on conductivity was quantified in series 1 by taking thermal conductivity measurements on each sample at each V_f, over three successive cycles of compaction and unloading. Dry samples in test series 2 were tested at a single V_f value in each case given their relatively high stiffness in the through-thickness direction.

Various textile reinforcements were tested in the four successive steps of this work. Test series 1 probed the effects of textile architecture, V_f, successive compaction and vacuum on λ_{rip} and λ_{rtt} for two reinforcements made from Toho Tenax HTS40 PAN-based carbon fibres. Reinforcement stack 1.1 consisted of six layers of 534 g m^{-2} non-crimp stitched ±45° bidirectional reinforcement produced by Saertex from 12 K yarn. Reinforcement stack 1.2 consisted of 16 layers of 215 g m^{-2} 2 × 2 balanced twill-woven reinforcement produced by Texonic from 3 K yarn. Composites were produced from the same stacks with λ_{cip} and λ_{ctt} measured for comparison purposes, using resin R1 which is identified below.

Test series 2 quantified the effects of textile architecture, reinforcement thickness and yarns made of different fibres extending along the thickness on λ_{rip} and λ_{rtt} measured on 3D woven reinforcement fabrics. In all cases, composite plates were produced from the same reinforcement with λ_{cip} and λ_{ctt} measured for comparison purposes, using resin R2 as identified below. In view of the relatively high transverse stiffness of the 3D woven reinforcements, tests performed on dry reinforcements and composites were conducted at single nominal V_f values for each material and case; the effect of V_f was not probed. Reinforcement 2.1 was a monolithic 3D woven carbon reinforcement featuring 3 K and 12 K yarns of Toho Tenax HTS40 PAN-based carbon fibres balanced along the warp and weft, with 1% carbon z-fibre binding yarns extending from the top surface to the bottom surface hence interlocking all
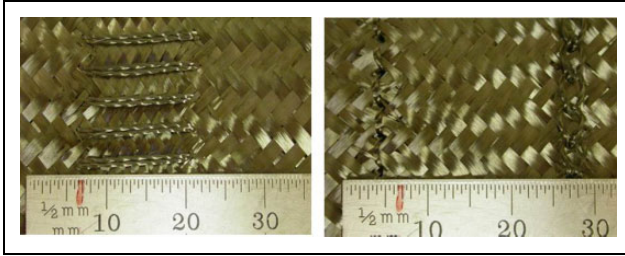
Figure 2. Face and rear views of one-sided stitch line used in twill carbon fibre stack 3.1 assembled using carbon fibre one-sided stitching.

in-plane yarns. The reinforcement was designed and made by Texonic and Centre des Technologies Textiles, St-Hyacinthe, QC, Canada, and had a surface density of 2541 g m^{-2}. Dry and composite samples averaged 3.12 and 2.72 mm in thickness, respectively, for nominal V_f values of 46.3% in the dry and 53.1% for the composite. Reinforcements 2.2 and 2.3 were two monolithic 3D woven hybrid carbon/glass reinforcements made from 12 K yarns of Hexcel IM7 PAN-based carbon fibres balanced along the warp and weft, with 5.6% S2 glass z-fibre binding yarns extending from the top surface to the bottom surface hence interlocking all in-plane fibres. Both reinforcements were acquired under contract from Albany Engineered Composites and provided by the US Army Research Laboratory. Thinner reinforcement 2.2 and thicker reinforcement 2.3 had surface densities of 3425 and 6165 g m^{-2}, respectively. Dry and composite samples made from reinforcement 2.2 averaged 4.37 and 4.13 mm in thickness leading to nominal V_f values of 44.0% in the dry and 46.5% for the composite, while dry and composite samples made from reinforcement 2.3 averaged 6.56 and 6.46 mm in thickness leading to nominal V_f values of 52.3% in the dry and 53.6% for the composite.

Test series 3 probed the effect on λ_{rip} and λ_{rtt} of one-sided stitching applied to a 20-layer stack of aforementioned 215 g m^{-2} 2 × 2 balanced twill-woven reinforcement produced by Texonic from 3 K yarn through its entire thickness, using a structural 134 tex twisted carbon thread. Stacks were thermally isotropic in-plane. Stitching as shown in Figure 2 was done at Centre des Technologies Textiles, St-Hyacinthe, QC, Canada, using a one-sided Keilmann RS 530 stitching head with 25.4 mm stitch width and 4.0 mm stitch pitch. Reinforcement stack 3.1 was assembled with a single stitch line extending along its 110 mm length, centred in the width of samples, and tested at different Vf values. Tests were not performed on composites in this case.

Test series 4 probed the effects of V_f on λ_{rip} and λ_{rtt} for one glass fibre reinforcement aiming at providing a general comparison with results obtained for the carbon fibre reinforcements tested in series 1 to 3. Reinforcement stack 4.1 consisted of eight layers of 305 g m^{-2} 2 × 2 balanced twill E glass woven reinforcement. Composites with an average

thickness of 1.86 mm and V_f of 53.5% were produced from the same stacks with λ_{cip} and λ_{ctt} measured for comparison purposes, again using resin R2.

Resin R1 was neat epoxy AKD/LEO 2376 supplied in 120 μm film by Axson. Composites made from non-crimp stitched and woven reinforcements in step 1 were manufactured by RFI in a PF120 Carbolite oven. Fabrics and resin film were intercalated, vacuum bagged and processed at 2°C min^{-1} to 130°C, dwell for 2 h, ramp at 2°C min^{-1} to 200°C and dwell for 2 h. Void fractions in the plates were well below 1%, consistently. Resin R2 was liquid epoxy West System 105/206 slow hardener with a 5:1 ratio. Composites made from 3D woven reinforcements in step 2 and woven E glass reinforcements in step 4 were manufactured using vacuum-assisted resin transfer moulding under full vacuum between cast aluminium plates, and cured at room temperature. Void fractions were similar to those reported above.

Variability of devices and data

Variability of the THISYS and THASYS devices for measurements taken at 20°C are quoted by the manufacturer as ±2% and ±1%, respectively. Two types of variability for both in-plane and through-thickness thermal conductivity data were quantified: variability of the THISYS and THASYS devices, and total variability of the data. Variability refers to the ratio of the standard deviation to the average of relevant data.

In test series 1, device variability was calculated based on two or three measurements: the original data value and either one or two repeated measurements performed on the same sample and at the same V_f, taken successively without removing samples from the devices. Data variability was calculated based on four measurements: the original value measured using the original sample and three more values measured using different samples at the same V_f; hence data variability includes variability of the device, variability due to differences in mounting the samples and inserts, as well as variability due to differences in preparation of the four samples. In test series 1, device variability was generally lower than 1% except for variability of THASYS evaluated with the vacuumed reinforcement stack 1.1 which stood at 2.8%. Total variability on conductivity data ranged from 6.7% to 11.2% for dry reinforcement samples tested at the same V_f and below 5% for composites, both in-plane and through-thickness. Results from test series 2 were very reproducible with values of the total variability mostly below 5%. Values of the total variability for composites were mostly below 1% while those of dry reinforcements were above 1%; variability was higher for the conductivity of dry reinforcements measured in the through-thickness direction λ_{rtt} with values of 4.3%, 8.3% and 6.3% for reinforcements 2.1, 2.2 and 2.3, respectively. Values of the total variability obtained in test series 3 were almost always below 1% for conductivities measured in the in-plane and

through-thickness directions, for carbon stacks featuring one-sided stitching and those devoid of stitching, as well as for glass dry stacks and composites, with no notable outliers. The same was observed with test series 4 performed on glass reinforcement 4.1 though in that case, fluctuations with V_f were far larger and the relation less clear.

Effect of release film

The effect of the Dahlar® release film used for preparing dry samples on measured in-plane and through-thickness thermal conductivities was quantified. In-plane thermal resistance R_{mip} of a material sample of thickness t_m and in-plane conductivity λ_{mip} is

$$R_{\text{mip}} = \frac{L}{\lambda_{\text{mip}} \cdot w t_m} \quad (3)$$

where L is heat flux length and w is sample width. Combining with two in-plane thermal resistances R_{fip} from both release film layers with identical L and w leads to apparent in-plane thermal resistance R_{aip}

$$R_{\text{aip}} = \frac{1}{\frac{1}{R_{\text{mip}}} + \frac{2}{R_{\text{fip}}}} \quad (4)$$

Knowing the thickness t_f and thermal conductivity of the film λ_{fip}, total thickness t_a and the apparent thermal conductivity λ_{aip} measured for the material sample and films leads to λ_{mip} for the material sample

$$\lambda_{\text{aip}} = \frac{\lambda_{\text{mip}} t_m + 2\lambda_{\text{fip}} t_f}{t_a} \quad (5)$$

Hence, λ_{mip} and λ_{aip} may be compared if λ_{fip} is known. Similarly, through-thickness thermal resistance R_{mtt} of a material sample of thickness t_m and through-thickness conductivity λ_{mtt} is:

$$R_{\text{mtt}} = \frac{t_m}{\lambda_{\text{mtt}} A} \quad (6)$$

where A is the area normal to the heat flux. Adding two through-thickness thermal resistances R_{ftt} from both release film layers with identical A leads to apparent through-thickness thermal resistance R_{att}

$$R_{\text{att}} = R_{\text{mtt}} + 2R_{\text{ftt}} \quad (7)$$

Knowing the thickness t_f and thermal conductivity of the film λ_{ftt}, total thickness t_a and the apparent thermal conductivity λ_{att} measured for the material sample and films leads to λ_{mtt} for the material sample

$$\lambda_{\text{att}} = \frac{t_a}{\frac{t_m}{\lambda_{\text{mtt}}} + 2\frac{t_f}{\lambda_{\text{ftt}}}} \quad (8)$$

hence λ_{mtt} and λ_{att} may also be compared. A thermal conductivity $\lambda_{\text{fip}} = \lambda_{\text{ftt}}$ of 0.2 W m^{-1} K^{-1} was obtained from more than 20 in-plane and transverse measurements performed on single sheets and stacks of Dahlar® 50 μm thick

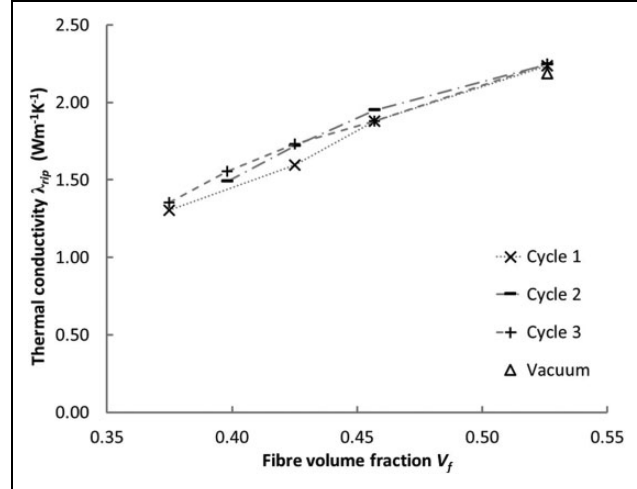**Figure 3.** In-plane thermal conductivity λ_{rip} of six layers non-crimp carbon fibre reinforcement stack 1.1.
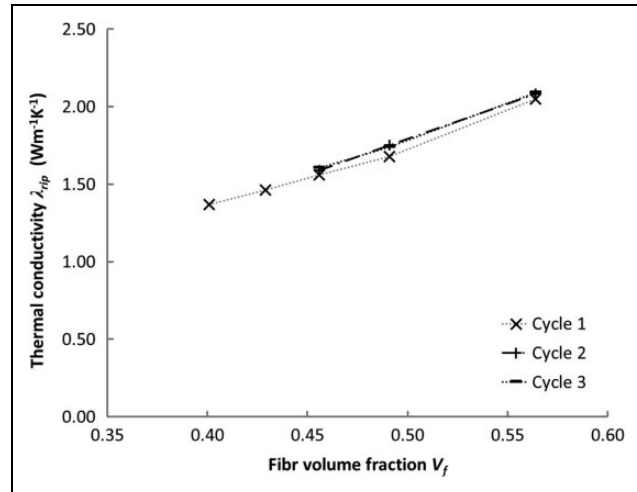
Figure 4. In-plane thermal conductivity λ_{rip} of six layers balanced twill-woven carbon fibre reinforcement stack 1.2.

release film; isotropic thermal behaviour was assumed henceforth for the film. The conservative estimates of $\lambda_{\text{rip}} = 1$ W m^{-1} K^{-1} and $\lambda_{\text{rtt}} = 0.1$ W m^{-1} K^{-1} from the literature along with $t_m = 3.0$ mm from apparatus configuration lead to underestimates of less than 1% for λ_{rip} and negligible for λ_{rtt}; differences are more significant for λ_{cip} and λ_{ctt} as composites are more conductive, but Dahlar® film was not used when taking measurements on solid composites with reinforcements saturated with cured epoxy resin.

Results

Series 1: Effect of textile architecture, V_f, de-bulking and vacuum

Results obtained from thermal conductivity measurements performed on reinforcement stacks 1.1 and 1.2 appear in Figures 3 to 8. In the in-plane direction, Figures 3 and 4
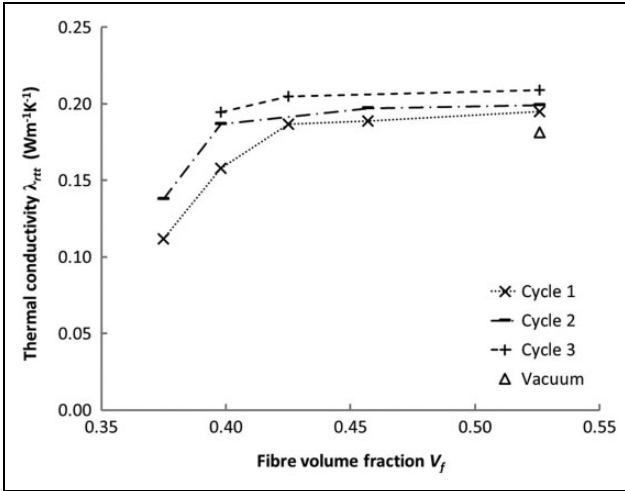
Figure 5. Through-thickness thermal conductivity λ_{rtt} of six layers non-crimp carbon fibre reinforcement stack 1.1.
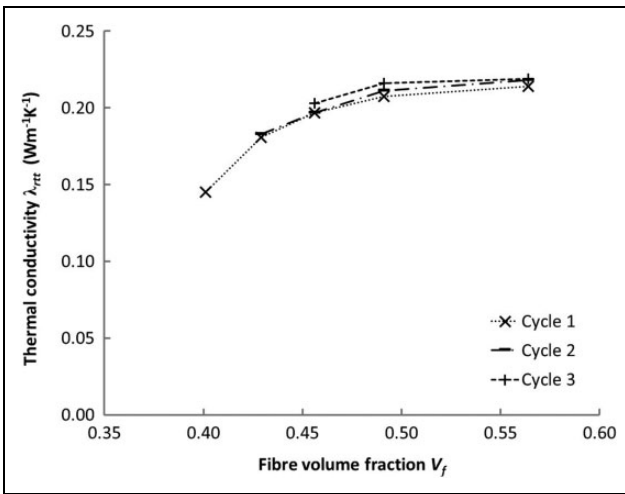

Figure 6. Through-thickness thermal conductivity λ_{rtt} of six layers balanced twill-woven carbon fibre reinforcement stack 1.2.
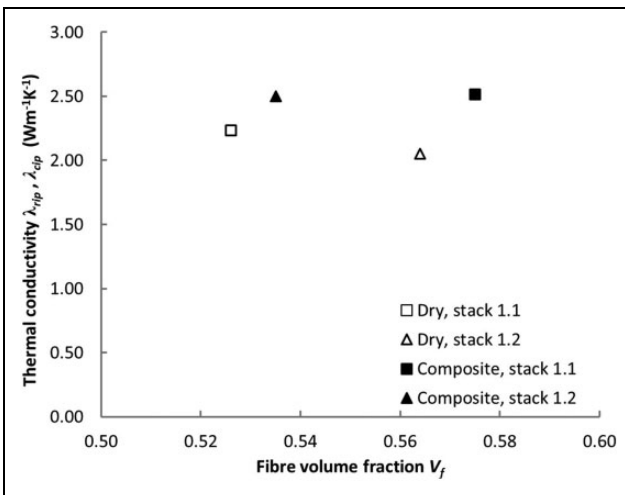

Figure 7. In-plane thermal conductivity of dry reinforcements λ_{rip} and composites λ_{cip}, six layers non-crimp carbon fibre and six layers balanced twill-woven carbon fibre reinforcement stacks 1.1 and 1.2.
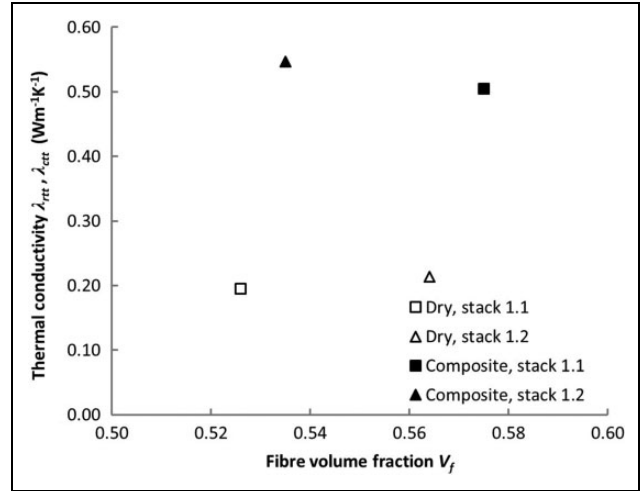
Figure 8. Through-thickness thermal conductivity of dry reinforcements λ_{rtt} and composites λ_{ctt}, six layers non-crimp carbon fibre and six layers balanced twill-woven carbon fibre reinforcement stacks 1.1 and 1.2.
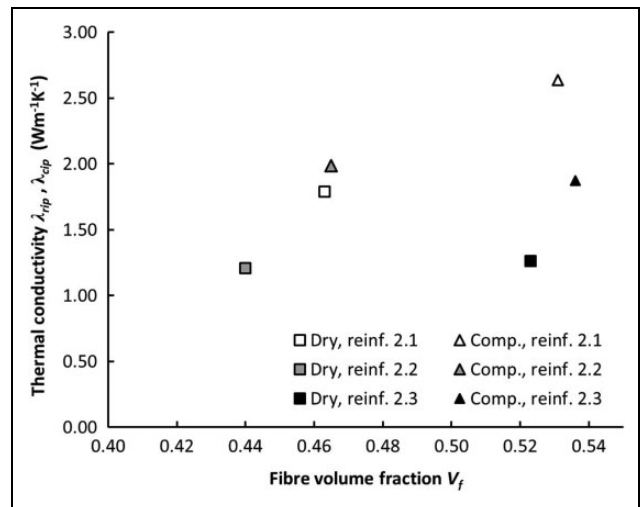
Figure 9. In-plane thermal conductivity of dry reinforcements λ_{rip} and composites λ_{cip}, 3D woven reinforcement stacks 2.1, 2.2 and 2.3 featuring structural carbon fibres. 3D: three-dimensional.

show that λ_{rip} for both reinforcement stacks varies linearly as a function of V_f. The non-crimp and twill reinforcements showed similar in-plane conductivities ranging from 1.303 W m^{-1} K^{-1} to 2.249 W m^{-1} K^{-1} for non-crimp stack 1.1 and from 1.367 W m^{-1} K^{-1} to 2.092 W m^{-1} K^{-1} for twill stack 1.2. The λ_{rip} values for non-crimp stack 1.1 were slightly higher than the values for twill stack 1.2 at the same V_f. A mild but consistent effect of successive compaction cycles is seen for both reinforcements, with values measured at the same V_f increasing slightly after each cycle. Vacuumed non-crimp stack 1.1 returned a value of 2.188 W m^{-1} K^{-1} at 52.6% V_f; 2.4% lower than that of its non-vacuumed counterpart.

In the through-thickness direction, Figures 5 and 6 show that λ_{rtt} for both reinforcements follows an exponential
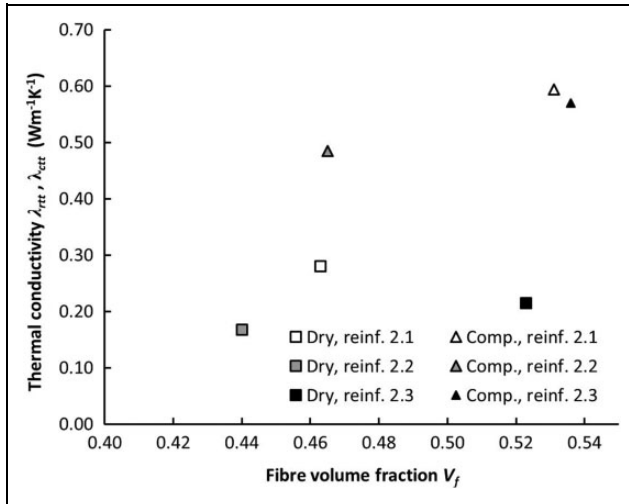
Figure 10. Through-thickness thermal conductivity of dry reinforcements λ_{rtt} and composites λ_{ctt}, 3D woven reinforcement stacks 2.1, 2.2 and 2.3 featuring structural carbon fibres. 3D: three-dimensional.
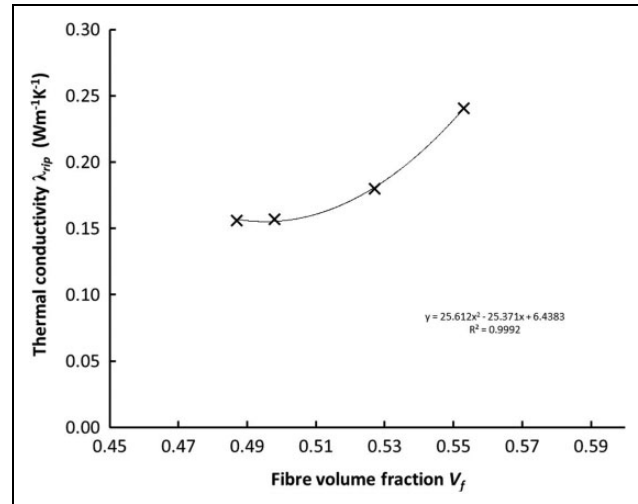

Figure 12. Through-thickness thermal conductivity of dry reinforcements λ_{rtt} of 20 layers balanced twill-woven carbon fibre reinforcement stack 3.1 assembled using one-sided carbon fibre structural stitch.
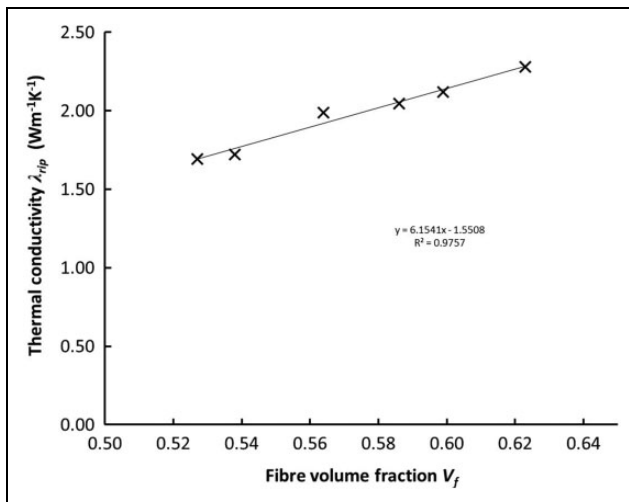

Figure 11. In-plane thermal conductivity of dry reinforcements λ_{rip} of 20 layers balanced twill-woven carbon fibre reinforcement stack 3.1 assembled using one-sided carbon fibre structural stitch.
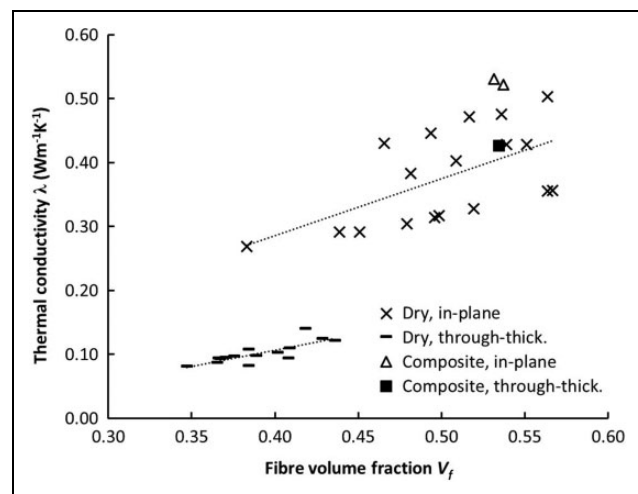

Figure 13. Thermal conductivities of dry reinforcements and composites of eight layers balanced twill-woven E glass fibre reinforcement stack 4.1.

recovery trend as a function of V_f. Both reinforcements showed conductivities in comparable ranges; values ranged from 0.112 W m^{-1} K^{-1} to 0.209 W m^{-1} K^{-1} for non-crimp stack 1.1 and from 0.145 W m^{-1} K^{-1} to 0.219 W m^{-1} K^{-1} for twill stack 1.2. The λ_{rtt} values for the non-crimp reinforcement were very similar to the values for the twill reinforcement at the same V_f. The effect of successive compaction cycles was seen with both reinforcements; amplitude was stronger in the through-thickness than for the in-plane case. Vacuumed non-crimp stack 1.1 returned a value of 0.182 W m^{-1} K^{-1} at 52.6% V_f, 7.4% lower than that of its non-vacuumed counterpart.

Thermal conductivity data for two composites made from both reinforcement stacks were compared with those

of the dry reinforcements in the in-plane and through-thickness directions, Figures 7 and 8. Composite plates made using stacks 1.1 and 1.2 showed V_f values of 57.5% and 53.5%, respectively, while V_f values for the dry reinforcements used for comparison were 52.6% and 56.4%, respectively. In the in-plane direction, λ_{cip} and λ_{rip} for stack 1.1 were 2.499 and 2.236 W m^{-1} K^{-1}, respectively, while values for stack 1.2 were 2.513 and 2.050 W m^{-1} K^{-1}, respectively. Similar comparisons made for the through-thickness data show more significant differences; λ_{ctt} and λ_{rtt} for stack 1.1 were 0.547 and 0.195 W m^{-1} K^{-1}, respectively, while values for stack 1.2 were 0.505 and 0.214 W m^{-1} K^{-1}, respectively. The in-plane to through-thickness thermal conductivity ratio was approximately
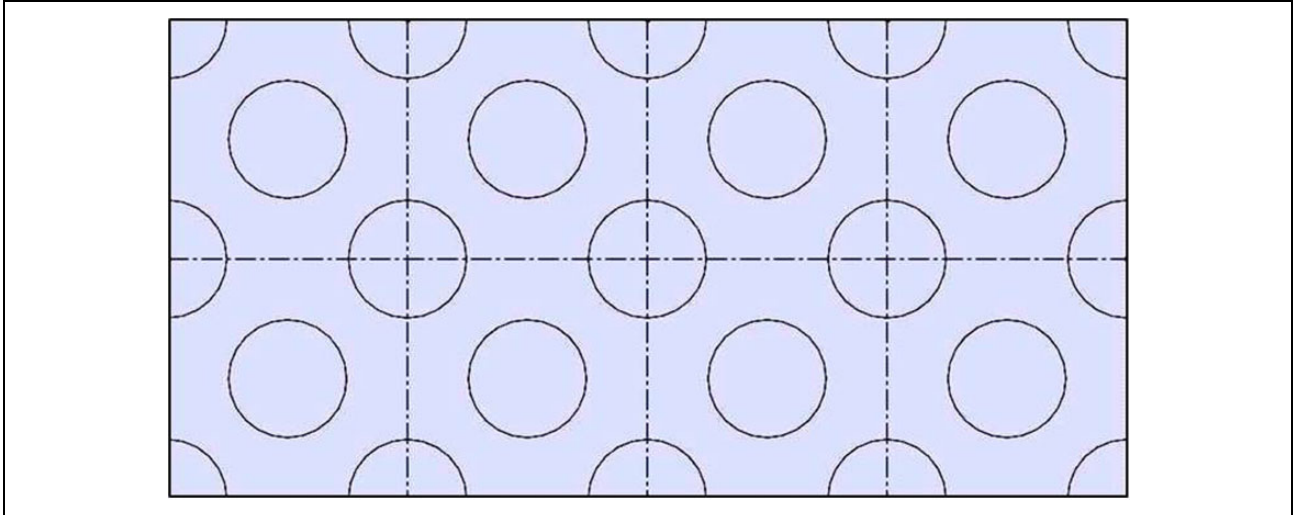
Figure 14. Typical geometry for SimNC simulations.

5 for the carbon fibre-epoxy composites compared to approximately 10 for the dry carbon fibre reinforcements, the latter approaching values typically reported for carbon fibres.

Series 2: 3D woven reinforcements

Results obtained from thermal conductivity measurements performed on reinforcements 2.1, 2.2 and 2.3 and their composites appear in Figures 9 and 10. Both in-plane and through-thickness conductivity values measured for 3D woven reinforcements and their composites compared generally with those obtained for stacks 1.1 and 1.2. In-plane values obtained for composites are somewhat larger than those measured with the dry reinforcements as reported above, while a significant difference is observed through-thickness. Here again, in-plane conductivity values are systematically larger than through-thickness values by a factor of approximately 10. Interestingly, the effect of V_f was muted for 3D weaves; although structures of reinforcements 2.1, 2.2 and 2.3 were not entirely similar, reduced differences in both conductivities at different V_f may result from superimposed yarns being much better aligned in 3D weaves as opposed to stacks 1.1 and 1.2 as a result of the manufacturing process.

Series 3: Through-thickness one-sided stitching using carbon thread

Results obtained from measurements performed on reinforcement stack 3.1 appear in Figures 11 and 12. In-plane conductivity was not affected by the presence of one-sided stitching as values presented in Figure 12 replicate those presented in Figure 4 for reinforcement 1.2. Conversely, while the range of through-thickness conductivity values presented in Figure 12 was essentially unchanged and orthotropy ratios remained largely similar, an inversion in
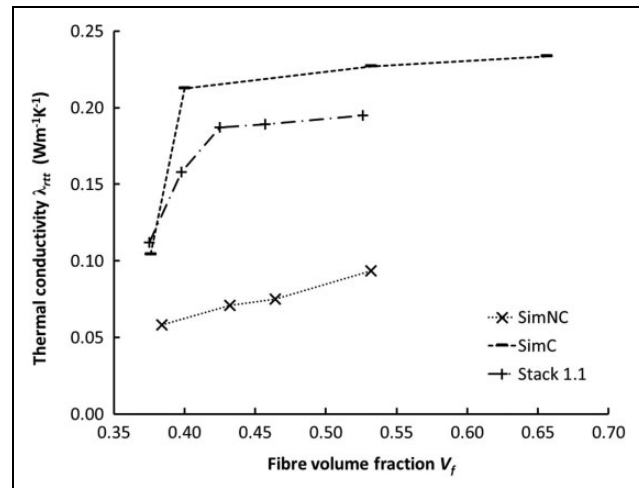

Figure 15. Results of SimNC and SimC simulations with experimental λ_{rtt} results, stack 1.1 (cycle 1).

trend was observed for the effect of V_f. In this case, zones of reinforcement stacks under stitching lines will undergo more compression while contact with THASYS platens may be reduced in zones immediately surrounding the stitching lines. One may conclude that through-thickness one-sided stitching with carbon thread does affect the local heat transfer through stacks of carbon reinforcements.

Series 4: Glass fibre reinforcements

Results obtained from measurements conducted on reinforcement stack 4.1 and its composite appear in Figure 13. Similar observations can be made. Values of in-plane conductivity for the dry reinforcement are larger for in-plane λ_{rip} than for through-thickness λ_{rtt} even as glass fibres are likely closer to thermal isotropy, as a result of the textile reinforcement structure. In-plane and through-thickness conductivity values for the composite λ_{cip} and λ_{ctt} are
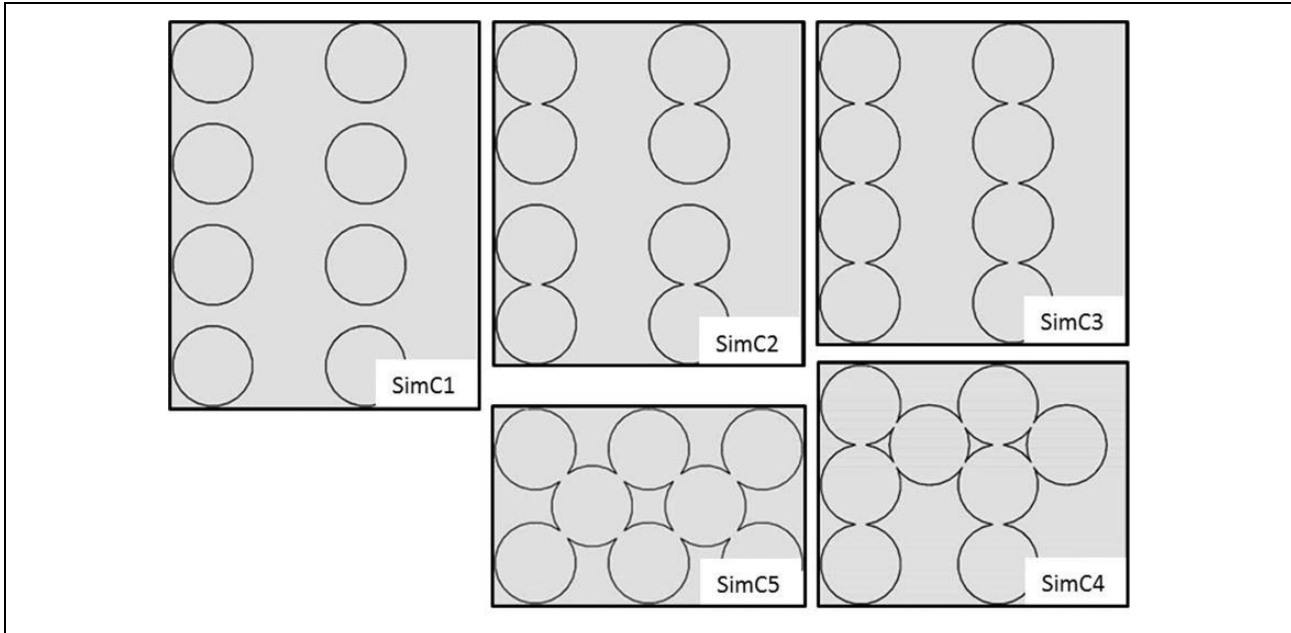
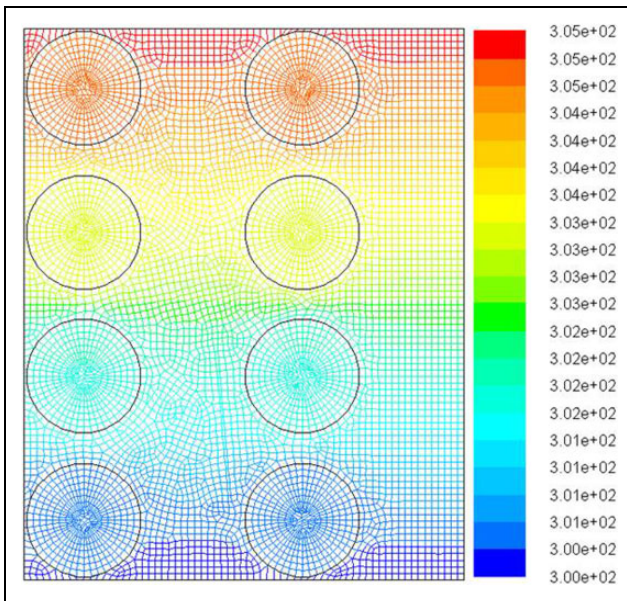**Figure 16.** Geometries SimC1 to SimC5 for SimC simulation series.

Figure 17. Mesh and temperature distribution, SimC1 (K).

closer, and conductivity values measured for the dry reinforcement and composite are also closer as a result of closer conductivities of the base materials. Still, the effect of resin on conductivity is more marked along the thickness. It is well worth noting that while in-plane conductivities of dry glass reinforcement 4.1 and its composite are clearly lower than those of dry carbon reinforcements and composites measured in this work, the same cannot be said of through-thickness conductivities. Hence, the kinetics of through-thickness heat transfer through dry preforms in processes such as RFI will not differ to the extent that may

be expected if considering only the thermal conductivity of the constituent fibres along their axial direction.

Discussion

The linear effect of V_f on λ_{rip} was expected from the rule of mixtures. Conversely, the exponential recovery trend on λ_{rtt} was unexpected. Hind and Robitaille[8] reported broadly exponential trends from Clayton's model[10] applied to composites. No analytical or semi-empirical models of the through-thickness thermal conductivity of textiles were found in the literature, hence this was probed. Two-dimensional (2D) steady-state simulations were performed using FLUENT ANSYS 13.0 in an attempt to replicate the trend on λ_{rtt}. The simulations did not account for reinforcement architecture based on the limited differences in data measured for stacks 1.1 and 1.2. Simulation results were compared with data measured for stack 1.1. Heat transfer in dry fabrics was assumed to occur primarily through conduction; air convection in the samples was assumed to be negligible. Constant temperatures were imposed on top and bottom domain walls while side walls were set as adiabatic. The through-thickness thermal conductivity λ_{rtt} was calculated using Fourier's law based on the average of the resulting heat flux measured at the top and bottom boundaries, which were always consistent within 5%.

A first group of simulations that did not model contacts between fibres were referred to as SimNC. Equally spaced and regularly aligned fibres of circular cross sections surrounded by air were represented by square unit cells, Figure 14. Eight unit cells were used in each simulation. Four cases were run with V_f values ranging from 38.0% to 53.0%. Diameter of the fibres was set to 7 μm.[29] V_f was
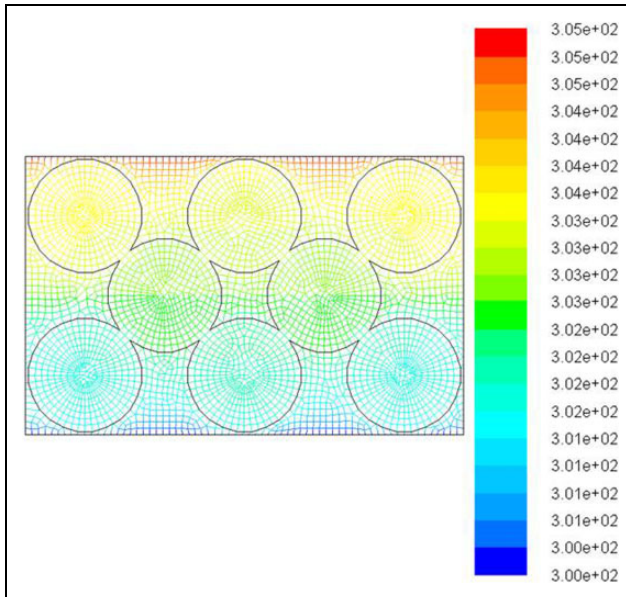
Figure 18. Mesh and temperature distribution, SimC5 (K).

increased by reducing the height and width of each unit cell hence reducing the distance between adjacent fibres. Constant temperatures were imposed to the top and bottom walls of the domain while side walls were adiabatic. The through-thickness thermal conductivity λ_{rtt} was calculated using Fourier's law based on the average heat flux on the top and bottom boundaries which were consistent within 5%. SimNC simulation results presented in Figure 15 ranged from 0.058 W m^{-1} K^{-1} to 0.095 W m^{-1} K^{-1} and could not replicate the exponential trend observed experimentally.

It was suspected that SimNC simulations underestimated λ_{rtt} values due to the lack of fibre contacts providing paths for heat conduction. A second group of 2D steady-state simulations referred to as SimC and featuring contacts were performed in FLUENT, using otherwise identical conditions. Five cases, SimC1 to SimC5, were run with V_f ranging from 33.4% to 65.8%, Figure 16. The cases offer a simplified representation of contacts between adjacent fibres developing during compaction. SimC1 represents an initial state where contacts between fibres are limited. Additional contacts develop in SimC2 and SimC3 where direct paths for conduction in the through-thickness appear, reducing the reliance of heat transfer through air. Fibres shift in SimC4 as a result of further compaction, connecting more heat paths; the network is further enhanced in SimC5. While the cases represent five possible local configurations among a wide array of alternatives, they aim at modelling incremental changes in fibre contacts with increasing V_f. SimC simulation results appear in Figure 15 along with SimNC simulation results and experimental data for stack 1.1. SimC simulations featuring fibre contacts yielded reasonable predictions for λ_{rtt} of dry fabrics and replicated the exponential recovery trend seen with measured data. Plots showing temperature distributions appear in Figures 17 and 18.

Conclusion

Reproducible values of λ_{rip} and λ_{rtt} were obtained for reinforcements. Orthotropy ratios quoted in the literature were validated. The effects of de-bulking and vacuum were quantified. Limited differences were seen between the in-plane conductivities for reinforcements and composites made from the reinforcements; conversely, the through-thickness conductivities for reinforcements were markedly lower than those of composites. Textile structures were found to affect properties. The in-plane conductivities of non-crimp reinforcements were marginally larger while the through-thickness conductivities of weaves were marginally higher. 3D weaving had limited impact on conductivity while one-sided through-thickness stitching affected the relationship between λ_{rtt} and V_f. Differences in λ_{rtt} for glass and carbon fabrics were markedly lower than one may have expected. The above is useful for process engineering as the through-thickness heat transfer can play a major role, say for RFI or consolidation with semi-pregs or featuring heavier ancillary materials.

Declaration of conflicting interests

The author(s) declared no potential conflicts of interest with respect to the research, authorship, and/or publication of this article.

ORCID iD

François Robitaille https://orcid.org/0000-0002-3463-5210

References

1. Yamane T, Katayama S, Todoki M, et al. The measurements of thermal conductivity of carbon fibres. *J Wide Bandgap Mater* 2000; 7(4): 294–305.
2. Heremans J, Rahim I and Dresselhaus MS. Thermal conductivity and Raman spectra of carbon fibers. *Phys Rev B* 1985; 32(10): 6742–6747.
3. Lee HJ and Taylor RE. Thermophysical properties of carbon/graphite fibers and MOD-3 fiber-reinforced graphite. *Carbon* 1975; 13(6): 521–527.
4. Pilling MW, Yates B and Black MA. The thermal conductivity of carbon fiber-reinforced composites. *J Mater Sci* 1979; 14(1): 1326–1338.
5. Dasgupta A, Agarwal RK and Bhandarkar SM. Three dimensional modeling of woven fabric composites for effective thermo-mechanical and thermal properties. *Compos Sci Technol* 1996; 56: 209–223.

6. Dasgupta A and Agarwal RK. Orthotropic thermal conductivity of plain-weave fabric composites using a homogenization technique. *J Compos Mater* 1992; 26(18): 2736–2758.

7. Glowania M, Lindner D, Linke M, et al. Influence of the pitch fiber reinforcement of CFRP on the mechanical and thermal conductivity properties. In: *Proceedings of the international conference on composite materials ICCM-18*, Jeju, South Korea, 21–26 August 2011, #96311.

8. Hind S and Robitaille F. Measurement, modeling, and variability of thermal conductivity for structural polymer composites. *Polym Compos* 2009; 31(5): 847–857.

9. Seo BH, Cho YJ, Youn JR, et al. Model for thermal conductivities in spun yarn carbon fabric composites. *Polym Compos* 2005; 26(6): 791–798.

10. Clayton WA. *Report: thermal conductivity of phenolic-carbon chars*. Chicago: Boeing Co, 1969.

11. Tsai SW and Hahn HT. *Introduction to composite materials*. Pennsylvania: Technomic Publishing, 1980.

12. Yoshihiro Y, Hiroaki Y and Hajime M. Effective thermal conductivity of plain weave fabrics and its composite material made from high strength fibers. *J Text Eng* 2008; 54(4): 111–119.

13. Matusiak M. Investigation of the thermal insulation properties of multilayer textiles. *J Fibre Text* 2006; 14(5): 98–102.

14. Onofrei E, Rocha AM and Catarino A. The influence of knitted fabrics' structure on the thermal and moisture management properties. *J Eng Fibre Fabric* 2011; 6(4): 10–22.

15. Matusiak M and Sikorski K. Influence of the structure of woven fabrics on their thermal insulation properties. *J Fibre Text* 2011; 19(5): 46–53.

16. Beckwith SW. Composites reinforcement fibers: III – the carbon and graphite families (part B). *SAMPE J* 2011; 47(3): 44–45.

17. Mortensen A. *Concise encyclopedia of composite materials*. The Netherlands: Elsevier, 2007, p.93–95.

18. Zweben C. Emerging high-volume applications for advanced thermally conductive materials. In: *Proceedings of the 49th international SAMPE symposium and exhibition*, Long Beach, CA, USA, 16–20 May 2004, pp.4061–4072.

19. Chung D. *Carbon fiber composites*. Massachusetts: Butterworth-Heinemann, 1994, p.9–10.

20. Dresselhaus MS, Dresselhaus G and Avouris P. *Carbon nanotubes: synthesis, structure, properties and applications*. Berlin, Germany: Springer-Verlag, 2001, p.21–23.

21. Hartary P, Hylton L and Zimmerman J. *Report: vapor grown carbon fibers*. Wheeling, USA: Missile Defense Agency – National Technology Transfer Center, Wheeling Jesuit University, 2008.

22. Hou J, Wang X and Zhang L. Thermal characterization of submicron polyacrylonitrile fibers based on optical heating and electrical thermal sensing. *Appl Phys Lett* 2006; 89(15).

23. Wei JX. *Report: carbon fiber thermal conductivity measurement and analysis*. Beijing Institute, Materials Science and Technology Division, 1989. China: Beijing Institute of Technology.

24. Katzman HA, Adams PM, Le TD, et al. Characterization of low thermal conductivity PAN-based carbon fibers. *Carbon* 1994; 32(3): 379–391.

25. Qiu L, Zheng XH, Zhu J, et al. The effect of grain size on the lattice thermal conductivity of an individual polyacrylonitrile-based carbon fiber. *Carbon* 2013; 51: 265–273.

26. Hexcel, HexTow IM 10 Carbon Fibre Product Datasheet, 2016. [Online]. Available: http://www.hexcel.com/Resources/DataSheets/Carbon-Fiber

27. Hexcel, HexTow IM 7 Carbon Fibre Product Datasheet, 2016. [Online]. Available: http://www.hexcel.com/Resources/DataSheets/Carbon-Fiber

28. Hexcel, HexTow AS 4 Carbon Fibre Product Datasheet, 2016. [Online]. Available: http://www.hexcel.com/Resources/DataSheets/Carbon-Fiber

29. Toho Tenax, Delivery Programme and Characteristics for Tenax HTS Filament Yarn, 2011. [Online]. Available: http://www.havel-composites.com/proddocs/HTS%20en%202011-04.pdf

30. Toray Composite Materials America Inc., TorayCA T300 Data Sheet, 2017. [Online]. Available: http://www.toraycfa.com/pdfs/T300DataSheet.pdf

31. Cytec Engineered Materials, Thornel T650/35 PAN Based Fiber Technical Data Sheet, 2012. [Online]. Available: http://www.cytec.com/products/thornel-t300?sp=eNpLsjVUS7Y1NDGyUMu1NbQwMAAAJaMD/w%3D%3D

32. Wetherhold RC and Wang J. Difficulties in the theories for predicting transverse thermal conductivity of continuous fiber composites. *J Compos Mater* 1994; 28(15): 1491–1498.

33. Bol'shakova NV, Kostenok OM, Il'in AM, et al. Thermal conductivity of carbon-graphite fibres and fabrics. *J Therm Eng* 1991; 9: 524–527.

34. Cytec Engineered Materials, Thornel 50 Carbon Fibre Properties Data Sheet. [Online]. Available: http://www.matweb.com/search/datasheet.aspx?matguid=855dacc29dbc4f46a4b17519dca89673&ckck=1

35. Uzun M. Ultrasonic washing effect on thermo physiological properties of natural based fabrics. *J Eng Fibre Fabric* 2013; 8(1): 39–51.

36. Xiaogang S, Jihong L and Sa L. Research on heat conduction performance of carbon-fibre fabric based on infrared thermal imaging technology. *Proc IEEE Int Sympos Knowledge Acquisit Model Workshop* 2008; 4(1): 40–43.

37. Ziaei M and Ghane M. Thermal insulation property of spacer fabrics integrated by ceramic powder impregnated fabrics. *J Industr Text* 2012; 43(1): 20–33.

38. Yamashita Y, Yamada H and Miyake H. Effective thermal conductivity of plain weave fabric and its composite material made from high strength fibers. *J Text Eng* 2008; 54(4): 111–119.

39. Cytec Engineered Materials, Thornel VCB-20 Carbon Fibre Cloth Data Sheet. [Online]. Available: http://www.matweb.com/search/datasheet.aspx?matguid=f0231febe90f4b45857f543bb3300f27

40. Hes L and Dolezal I. New method and equipment for measuring thermal properties of textiles. *J Text Mach Soc Japan* 1989; 42: T124–T127.